Computational method for the quantum Hamilton-Jacobi equation: One-dimensional scattering problems

Chia-Chun Chou and Robert E. Wyatt*
Institute for Theoretical Chemistry and Department of Chemistry and Biochemistry, The University of Texas at Austin, Austin, Texas 78712, USA

(Received 26 March 2006; revised manuscript received 26 September 2006; published 19 December 2006)

One-dimensional scattering problems are investigated in the framework of the quantum Hamilton-Jacobi formalism. First, the pole structure of the quantum momentum function for scattering wave functions is analyzed. The significant differences of the pole structure of this function between scattering wave functions and bound state wave functions are pointed out. An accurate computational method for the quantum Hamilton-Jacobi equation for general one-dimensional scattering problems is presented to obtain the scattering wave function and the reflection and transmission coefficients. The computational approach is demonstrated by analysis of scattering from a one-dimensional potential barrier. We not only present an alternative approach to the numerical solution of the wave function and the reflection and transmission coefficients but also provide a computational aspect within the quantum Hamilton-Jacobi formalism. The method proposed here should be useful for general one-dimensional scattering problems.

DOI: 10.1103/PhysRevE.74.066702 PACS number(s): 02.70.−c, 02.60.Lj, 03.65.Nk

I. INTRODUCTION

The quantum Hamilton-Jacobi formalism developed by Leacock and Padgett in 1983 provides an alternative approach to nonrelativistic quantum mechanics [1,2], and the detailed discussion of semiclassical forms and of the connection between this formalism and the WKB approximation has been presented [2]. In this approach, the quantum Hamilton-Jacobi equation (QHJE) with its accompanying physical boundary condition replaces the Schrödinger equation as the dynamical equation of a full Hamilton-Jacobi formalism of quantum mechanics. The solution to the QHJE, the quantum action variable, can be used to determine the bound state energy eigenvalues without explicitly solving the Schrödinger equation. This method has been applied to many one-dimensional bound state problems and separable problems in higher dimensions to obtain the energy eigenvalues and the bound state wave functions for solvable potentials [1–5]. The band edge eigenfunctions and eigenvalues for periodic potentials have also been determined by this formalism [6–8]. The connection between supersymmetric quantum mechanics and the quantum Hamilton-Jacobi formalism has been explored [9–12]. Furthermore, the quantum Hamilton-Jacobi formalism was found useful to provide not only information on the energy eigenvalues and the wave function but also the eigentrajectory of a particle in a given quantum state in complex phase space. Eigentrajectories in the complex space satisfying the QHJE have been studied for the free particle, the harmonic potential, and the hydrogen atom [13–17]. Besides, a computational method in the framework of Bohmian mechanics with complex action has been developed [18,19]. This method has been applied to the scattering problem of a Gaussian wave packet from an Eckart barrier. On the other hand, the quantum stationary Hamilton-Jacobi equation for bound stationary states has been explored in the trajectory representation in the real phase space through the bipolar decomposition of the wave function [20–24]. Moreover, the bipolar representation has been used to reconcile semiclassical mechanics and Bohmian mechanics [25–27].

In contrast to the many studies of bound systems, there are few studies devoted to scattering problems in the framework of the quantum Hamilton-Jacobi formalism. Trajectories and tunneling dynamics in the complex space for the potential step and for the potential barrier have been explored analytically [13,28]. In addition to the lack of exact analysis on scattering problems relating to quantum Hamilton-Jacobi theory, no computational approach for these problems has been proposed to numerically obtain the quantum momentum function (QMF) and the wave function from the QHJE. The purpose of this study is to present a computational method for one-dimensional scattering problems. The Möbius propagation scheme will be used to numerically solve the Riccati-type QHJE for the QMF [29]. We numerically integrate the QHJE backwards for the QMF from a large positive initial point in the transmitted region. Furthermore, the reflection and transmission coefficients are determined from the QMF and the scattering wave function is synthesized through the phase integral. In this paper, we not only present an alternative approach to the numerical solution of the wave function and the reflection and transmission coefficients but also provide a computational aspect within the quantum Hamilton-Jacobi formalism.

This paper is organized as follows. We begin by briefly reviewing the concepts of the quantum Hamilton-Jacobi formalism in Sec. II. In Sec. III, the exact analysis for the QMF for barrier scattering is presented. The significant differences in the pole structure of the QMF between scattering and bound state wave functions are described. In Sec. IV, an accurate computational method for general scattering problems is described to numerically obtain the QMF and the scattering wave function; moreover, these computational procedures are demonstrated by analysis of scattering from one-dimensional potential barriers. We also compare the results

*Electronic address: wyattre@mail.utexas.edu

obtained from our method with those obtained from the Numerov method. Finally, some remarks are given and we conclude in Sec. V with a discussion of the proposed numerical method for solving the QHJE.

II. QUANTUM HAMILTON-JACOBI FORMALISM

The quantum Hamilton-Jacobi equation is readily obtained by substituting the complex-valued time-dependent wave function in polar form, $\Psi(x,t)=\exp[iS(x,t)/\hbar]$, into the time-dependent Schrödinger equation

$$-\frac{\partial S}{\partial t}=\frac{1}{2m}\left(\frac{\partial S}{\partial x}\right)^2+V(x)+\frac{\hbar}{2mi}\frac{\partial^2 S}{\partial x^2}, \tag{1}$$

where $S(x,t)$ is the complex action or Hamilton's principal function. We can separate out the time for states of definite energy E (eigenenergy) by writing $S(x,t)=W(x,E)-Et$, where $W(x,E)$ is the quantum characteristic function. The QMF $p(x,E)$ is defined through the quantum characteristic function by $p(x,E)=\partial W(x,E)/\partial x$. Using the QMF to rewrite the QHJE, we have

$$\frac{1}{2m}p(x,E)^2+V(x)+\frac{\hbar}{2mi}\frac{\partial p(x,E)}{\partial x}=E. \tag{2}$$

We can complete the definition of the QMF by imposing the physical boundary condition

$$\lim_{\hbar\to 0}p(x,E)=p_c(x,E), \tag{3}$$

where $p_c(x,E)$ is the classical momentum function defined by $p_c^2(x,E)=2m[E-V(x)]$. Furthermore, the QMF can be expressed through the action function by the time-independent wave function

$$p(x,E)=\frac{\hbar}{i}\frac{\partial}{\partial x}\ln\psi(x,E) \tag{4}$$

$$=\frac{\hbar}{i}\frac{1}{\psi(x,E)}\frac{\partial\psi(x,E)}{\partial x}. \tag{5}$$

The QMF is extended to the complex plane by regarding x as a complex variable. From this equation, nodes in the wave function correspond to poles of the QMF. The positions of these poles, called *moving poles* [3], are energy dependent.

III. QUANTUM MOMENTUM FUNCTION FOR SCATTERING STATES

In this section, we will analyze the QMF for scattering from a potential step. Because the wave functions for one-dimensional continuum states are complex valued, the structure of the QMF $p(x)$ is very different from that for one-dimensional bound states [1–3]. The pole structure for the potential step will be analytically and thoroughly examined in this section.

The potential energy for a potential step is

$$V(x)=\begin{cases}0, & x<0 \text{ (region 1)},\\ V_0, & x>0 \text{ (region 2)}.\end{cases}$$

The wave function can be easily obtained [30]. For the energy E larger than V_0, the wave function is given by

$$\psi_1(x)=e^{ik_1x}+S^{(-)}e^{-ik_1x}, \tag{6}$$

$$\psi_2(x)=S^{(+)}e^{ik_2x}, \tag{7}$$

where $k_1=\sqrt{2mE}/\hbar$ and $k_2=\sqrt{2m(E-V_0)}/\hbar$. The reflection and transmission coefficients are given by

$$R=|S^{(-)}|^2, \tag{8}$$

$$T=\frac{k_2}{k_1}|S^{(+)}|^2. \tag{9}$$

Applying the appropriate boundary conditions at $x=0$, we can solve for the coefficients

$$S^{(-)}=\frac{k_1-k_2}{k_1+k_2}, \tag{10}$$

$$S^{(+)}=\frac{2k_1}{k_1+k_2}. \tag{11}$$

Similarly, when $E<V_0$, the wave function is given by

$$\psi_1(x)=e^{ik_1x}+S^{(-)}e^{-ik_1x}, \tag{12}$$

$$\psi_2(x)=S^{(+)}e^{-k_2x}, \tag{13}$$

where $k_1=\sqrt{2mE}/\hbar$ and $k_2=\sqrt{2m(V_0-E)}/\hbar$. Applying the appropriate boundary conditions at $x=0$, we can solve for the coefficients

$$S^{(-)}=\frac{k_1-ik_2}{k_1+ik_2}, \tag{14}$$

$$S^{(+)}=\frac{2k_1}{k_1+ik_2}. \tag{15}$$

For this case, the reflection and transmission coefficients are $R=1$ and $T=0$, respectively.

A. QMF on the real x axis

We will now analyze the QMF for the wave function in region 1 on the real x axis. Substituting the wave function $\psi_1(x)$ into Eq. (5), we have the QMF given by

$$p(x)=\hbar k\frac{e^{ikx}-S^{(-)}e^{-ikx}}{e^{ikx}+S^{(-)}e^{-ikx}} \tag{16}$$

$$=\hbar k\frac{1-|S^{(-)}|^2+2i|S^{(-)}|\sin(2kx-\theta)}{1+|S^{(-)}|^2+2|S^{(-)}|\cos(2kx-\theta)}, \tag{17}$$

where $S^{(-)}=a+bi$, $\cos\theta=a/\sqrt{a^2+b^2}$, and $\sin\theta=b/\sqrt{a^2+b^2}$. Although any linear combination of the two linearly independent plane waves is still a solution to the time-

independent Schrödinger equation for the free particle, from Eq. (16) the QMF of a linear combination of the two linearly independent plane waves is not a linear combination of the QMFs of the separate plane waves.

Let $2kx-\theta=2kz$ and if z is real valued, the denominator of the QMF in Eq. (17) is non-negative:

$$1+|S^{(-)}|^2+2|S^{(-)}|\cos(2kz) \geqslant 1+|S^{(-)}|^2+2|S^{(-)}|(-1)$$
$$=(1-|S^{(-)}|)^2 \geqslant 0.$$

Therefore, the QMF has no poles on the real x axis unless $|S^{(-)}|=1$. Moreover, the minimum of the denominator of $p(x)$ occurs at the point z_0 such that $\cos(2kz_0)=-1$. We can expand the QMF given by Eq. (17) around the point z_0 to the second order in the displacement $(z-z_0)$, and then the real and imaginary parts of the QMF become

$$p_R(z)=\hbar k\frac{\phi(E)}{\chi(E)+k^2(z-z_0)^2}, \tag{18}$$

$$p_I(z)=\hbar k\frac{-k(z-z_0)}{\chi(E)+k^2(z-z_0)^2}, \tag{19}$$

where

$$\phi(E)=\frac{1-|S^{(-)}|^2}{4|S^{(-)}|}, \quad \chi(E)=\frac{(1-|S^{(-)}|)^2}{4|S^{(-)}|}.$$

The condition that the QMF has poles is $|S^{(-)}|=1$ and, when this happens, the QMF becomes pure imaginary. We suppose that $|S^{(-)}|$ is close to 1 and let $|S^{(-)}|=1-\delta$, where δ is a small number, and expand the constants including $|S^{(-)}|$ of the real and imaginary parts of the QMF to the leading order term in δ

$$\chi(E)\simeq\left(\frac{\delta}{2}\right)^2, \quad \phi(E)\simeq\left(\frac{\delta}{2}\right).$$

Then the approximate forms of the real and imaginary parts of the QMF near the point z_0 become

$$p_R(z)=\hbar k\frac{\sigma}{k^2(z-z_0)^2+\sigma^2}, \tag{20}$$

$$p_I(z)=\hbar k\frac{-k(z-z_0)}{k^2(z-z_0)^2+\sigma^2}, \tag{21}$$

where $\sigma=\delta/2$. On the other hand, we suppose that the exact pole of the QMF is at $x_0+i\varepsilon$, and the QMF near the pole has the approximate form:

$$p(x)=\frac{\hbar}{i}\frac{1}{x-(x_0+i\varepsilon)} \tag{22}$$

$$=\hbar\left[\frac{\varepsilon}{(x-x_0)^2+\varepsilon^2}+i\frac{-(x-x_0)}{(x-x_0)^2+\varepsilon^2}\right]. \tag{23}$$

These approximate forms, Eq. (20) and Eq. (21), remind us that the pole is complex but it is close to the real axis when the absolute value of the coefficient $S^{(-)}$ is close to 1. Because these poles are very close to the real x axis and *almost* form poles on the real x axis, this can be called a "*quasi-pole*."

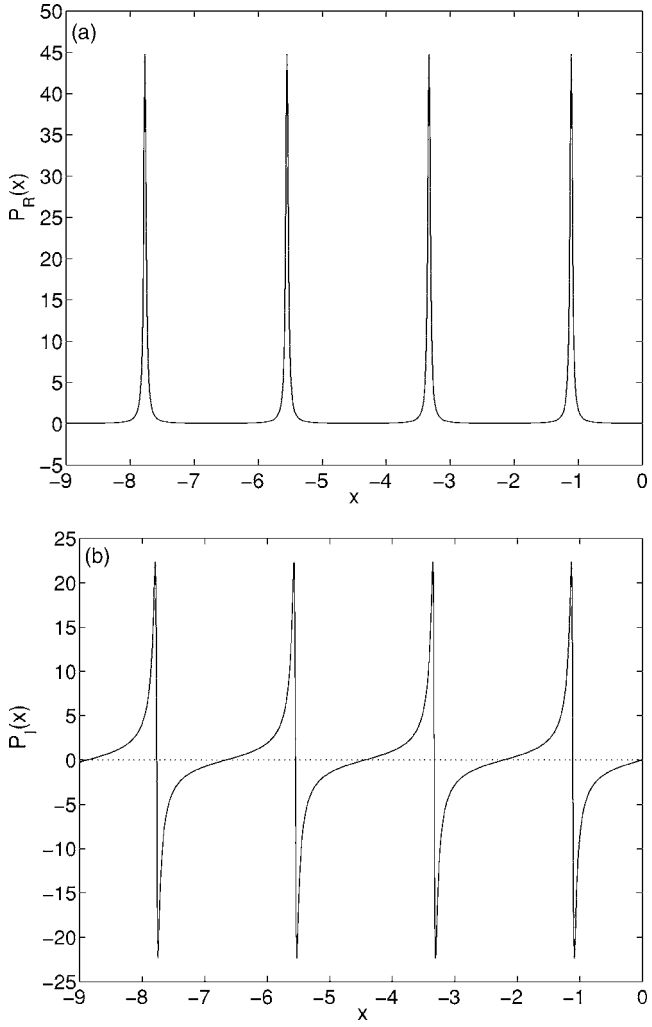

FIG. 1. Quantum momentum function for the potential step with the energy $E=1.001$ and $V_0=1$: (a) Real part; (b) imaginary part.

Next, we return to the potential step problem. For $E>V_0$, the QMF given in Eq. (17) reads

$$p(x)=\hbar k_1\frac{1-S^{(-)^2}+i2S^{(-)}\sin(2k_1x)}{1+S^{(-)^2}+2S^{(-)}\cos(2k_1x)}, \tag{24}$$

where $S^{(-)}$ is given by Eq. (10). In this case, we choose the energy E equal to 1.001 and the potential step V_0 equal to 1, and set $\hbar=m=1$. Figure 1 shows the real and imaginary parts of the QMF. When the energy E approaches V_0, the coefficient $S^{(-)}$ is close to 1. Then, as shown in Fig. 2, the approximate forms of the QMF given by Eq. (20) and Eq. (21) are in excellent agreement with the exact QMF. Actually, when $S^{(-)}$ is not equal to 1, the poles are in the complex x plane.

B. QMF in the complex x plane

We extend the QMF in Eq. (24) to the complex plane by regarding x as a complex variable. From Eq. (24), the QMF is the quotient of two analytic functions in the complex

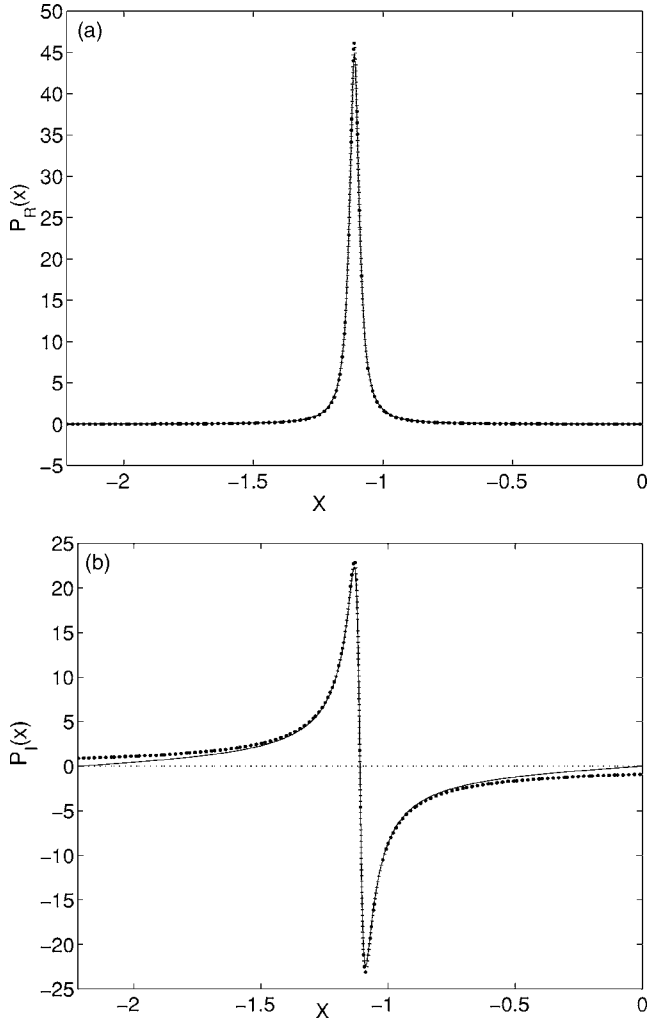

FIG. 2. Approximate form of the QMF (···) compared with the exact QMF (—) with the energy $E=1.001$ and $V_0=1$: (a) Real part; (b) imaginary part.

plane, so it is a *meromorphic* function [31]. The only possible poles are the zeros of the denominator, but a *common zero* of the numerator and denominator can also be a removable singularity. If this is the case, the value of the quotient must be determined by continuity.

The exact positions of the poles can be determined from the denominator of the QMF in Eq. (24) through the equation

$$1 + S^{(-)^2} + 2S^{(-)} \cos(2k_1 x) = 0. \tag{25}$$

Because $\cos\theta$ is a periodic function, the roots of this equation appear periodically and they are equal to $x=\alpha\pm i\beta$, where

$$\alpha = \frac{\pi - 2n\pi}{2k_1}, \tag{26}$$

$$\beta = \frac{1}{2k_1} \cosh^{-1}\left(\frac{1 + S^{(-)2}}{2S^{(-)}}\right), \tag{27}$$

and where $n=1,2,3,\ldots$, because $p(x)$ is defined in region 1 for $x<0$. Subsequently, we have to determine if these points

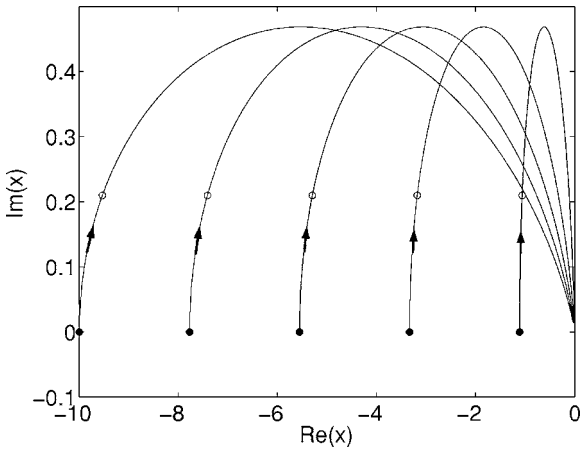

FIG. 3. Pole trajectories in the complex x plane from $E=1$ to $E=100\,000$ for the potential step $V_0=1$: $E=1$ (●) and $E=1.1$ (○).

$x=\alpha\pm i\beta$ are also the zeros of the numerator in Eq. (24). Substituting $x=\alpha-i\beta$ into the numerator, we find that they are also the zeros of the numerator. Therefore, through L'Hôpital's rule, we can obtain the limit of the indeterminant form of $p(x)$ and find that these points $x=\alpha-i\beta$ are *not* poles. These *artificial* poles come from the operation that we multiply the numerator and the denominator of $p(x)$ given in Eq. (16) by the complex conjugate of the denominator to obtain Eq. (17), and these points $x=\alpha-i\beta$ correspond to the zeros of the complex conjugate of the denominator. Actually, the only poles are at $x=\alpha+i\beta$.

For $E=1.001$ and $V_0=1$, one of the poles is at $x=-1.11017+0.02235i$. When the energy equals the potential step V_0, the coefficient $S^{(-)}$ given in Eq. (10) is equal to 1 and the poles form on the real x axis. Additionally, the wave function given in Eq. (6) becomes pure real and the QMF becomes pure imaginary. For the case $S^{(-)}=1$, from Eqs. (26) and (27), the exact positions of the poles are at $x=(\pi-2n\pi)/2k_1$ where $n=1,2,3,\ldots$ and there are an infinite number of poles on the real x axis. This feature of the QMF for the scattering wave function is very different from that for the bound state wave function. The QMF of the bound state wave function has a finite number of moving poles between the classical turning points [1–3]. For this scattering case, five poles on the real x axis are shown in Fig. 3. When the energy E increases, the poles deviate away from the real x axis. The five poles for $E=1.1$ and $V_0=1$ are also shown in Fig. 3. The arrows in this figure show the direction of these poles moving away from the real axis as the energy increases. Trajectories for the five poles are displayed in Fig. 3 for the energy range $E=1$ to $E=100\,000$ with the potential step $V_0=1$. From Eqs. (26) and (27), when the energy goes to infinity, all poles converge to the origin.

For $E<V_0$, the QMF is given by Eq. (17) with the coefficient $S^{(-)}=(k_1-ik_2)/(k_1+ik_2)$, where $k_2=\sqrt{2m(V_0-E)}/\hbar$. Because the absolute value of the coefficient $S^{(-)}$ is always equal to one, the QMF given by Eq. (17) is pure imaginary. Additionally, there are an infinite number of poles on the real x axis and their exact positions are determined by the equation

$$\cos(2k_1x - \theta) = -1. \tag{28}$$

From this equation, we can find that when the energy E becomes smaller, the separation between the poles of the QMF becomes larger. This feature is consistent with the phenomenon that the distance between the nodes of the wave functions for the potential step with $E < V_0$ increases when the energy of the incident particle goes to zero.

IV. COMPUTATIONAL METHOD FOR THE GENERAL SCATTERING PROBLEM

In this section, an accurate computational method will be presented to solve the general scattering problem through the QHJE. Since the wave function for large positive x approaches a plane wave traveling to the right, $\exp(ikx)$, the QMF goes like a constant $\hbar k$. Therefore, we numerically solve the QHJE *backwards* from a large positive value of x and the reflection and transmission coefficients are determined from the QMF.

A. Möbius propagation for Riccati differential equations

The QHJE in Eq. (2) is a version of the Riccati differential equation. The general form of the matrix Riccati equation for the solution matrix $y(x)$ is

$$\frac{dy}{dx} = a(x)y + b(x) - yc(x)y - yd(x), \tag{29}$$

where the unknown $y(x)$ is an $n \times m$ matrix function and the known coefficients $a(x)$, $b(x)$, $c(x)$, and $d(x)$ are $n \times n$, $n \times m$, $m \times n$, and $m \times m$ matrix functions, respectively. The QHJE in Eq. (2) is rewritten as

$$\frac{dp(x)}{dx} = \frac{i}{\hbar}[-p(x)^2 + 2m(E - V(x))], \tag{30}$$

where $p(x,E)$ has been replaced by $p(x)$.

Standard integration methods for differential equations fail to be successful for solving the Riccati differential equation, because they cannot accurately pass through singularities in the solution. Schiff and Shnider proposed a "natural approach" to the numerical integration of the Riccati differential equation in 1999 [29]. This method is based on the use of Möbius schemes, which makes it possible that the initial value problem, such as Eq. (2), can be accurately integrated even through singularities. For the general Riccati equation (29), the Möbius integrator has the form

$$y_{i+1} = (\tilde{\alpha}(x_i,h)y_i + \tilde{\beta}(x_i,h))(\tilde{\gamma}(x_i,h)y_i + \tilde{\delta}(x_i,h))^{-1}, \tag{31}$$

where y_i is an approximation to $y(x_i)$. The functions $\tilde{\alpha}(x_i,h)$, $\tilde{\beta}(x_i,h)$, $\tilde{\gamma}(x_i,h)$, and $\tilde{\delta}(x_i,h)$ are constructed from the coefficients $a(x)$, $b(x)$, $c(x)$, and $d(x)$ by

$$\tilde{\alpha}(x_i,h) = I_n + ha(x_i) + O(h^2),$$

$$\tilde{\beta}(x_i,h) = hb(x_i) + O(h^2),$$

$$\tilde{\gamma}(x_i,h) = hc(x_i) + O(h^2),$$

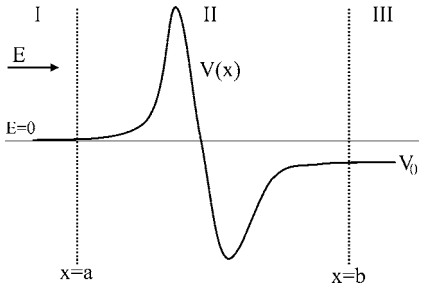

FIG. 4. General potential for scattering problems.

$$\tilde{\delta}(x_i,h) = I_m + hd(x_i) + O(h^2),$$

where I_n denotes the $n \times n$ identity matrix. The Möbius integrator in Eq. (31) shows how to construct an approximation y_{i+1} to $y(x_{i+1})$ from y_i, where $x_{i+1} = x_i + h$. The Möbius scheme can be constructed with arbitrary order.

Given the initial condition $p(x_0)$, the *first-order Möbius scheme* for the QHJE leads to the explicit one-step recursion relation

$$p(x_{k+1}) = \frac{p(x_k) + \frac{2mi}{\hbar}[E - V(x_k)]h}{\frac{i}{\hbar}p(x_k)h + 1}. \tag{32}$$

For small h, this recursion relation provides a qualitatively and quantitatively accurate solution through multiple singularities. In this study, the *second-order Möbius integrator*

$$p(x_{k+1}) = \frac{[1 - h^2(E - V(x_k))]p(x_k) + 2i[E - V(x_k)]h - ih^2V'(x_k)}{ip(x_k)h + [1 - h^2(E - V(x_k))]} \tag{33}$$

and the *fourth-order integrator* constructed from Eq. (33) in Ref. [29] will be used to obtain numerical solutions for $p(x)$.

B. Formulation of the scattering problem

A general potential for one-dimensional scattering problems is shown in Fig. 4. As in the general quantum mechanical method for scattering problems, we will first specify the appropriate asymptotic forms for the wave function at the energy E in regions I and III:

$$\psi_{\mathrm{I}}(x) = e^{ik_1x} + S^{(-)}e^{-ik_1x}, \tag{34}$$

$$\psi_{\mathrm{III}}(x) = S^{(+)}e^{ik_2x}, \tag{35}$$

where $k_1 = \sqrt{2mE}/\hbar$ and $k_2 = \sqrt{2m(E - V_0)}/\hbar$. For large positive x, the QMF approaches the constant real value $\hbar k_2$ because the exact wave function asymptotically becomes a plane wave traveling to the right. Then, we use this value as the initial condition for the QMF to *integrate backwards* from a large positive initial position using the Möbius propagation scheme. In general, the QMF is complex and we divide it into real and imaginary parts, $p(x) = p_R(x) + ip_I(x)$.

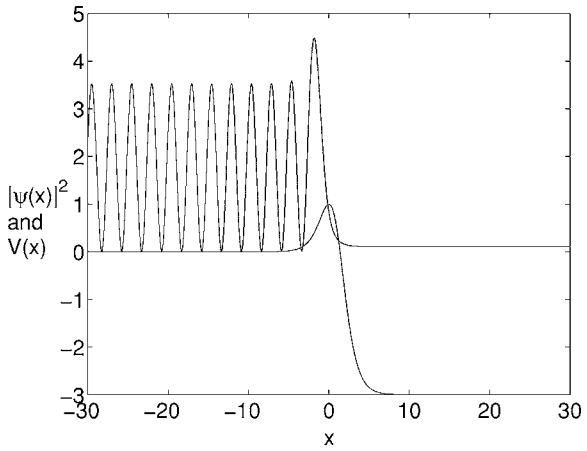

FIG. 5. Probability density (upper oscillating curve) and potential barrier ($c=0.5$). The incident energy is $E=0.8$ and the barrier height is $V_0=1$.

From Eq. (4), the wave function can be obtained through the phase integral

$$\psi(x) = \exp\left(\frac{i}{\hbar}\int p(x)dx\right)$$

$$= \exp\left(\frac{i}{\hbar}\int p_R(x)dx - \frac{1}{\hbar}\int p_I(x)dx\right). \quad (36)$$

From this equation, we find that the real part of the QMF contributes only to the phase of the wave function, while the imaginary part contributes only to the magnitude of the wave function. After obtaining the QMF numerically, we can synthesize the wave function through the phase integral in Eq. (36). It is important to note that if $p(x)$ has poles (for examples, for bound states), the phase integral must be correctly calculated by the *antithetic cancellation technique* so that the divergences on the two sides of the singularities can cancel each other [32,33].

When x goes to $-\infty$, the exact wave function approaches a linear combination of incoming and outgoing plane waves expressed by

$$\psi(x) = N[e^{ik_1x} + S^{(-)}e^{-ik_1x}], \quad (37)$$

where N is a constant and $k_1=\sqrt{2mE}/\hbar$. The reflection coefficient can be determined through this asymptotic form. Substituting Eq. (37) into the definition of the QMF in Eq. (4), we have

$$p(x) = \hbar k_1 \frac{e^{ik_1x} - S^{(-)}e^{-ik_1x}}{e^{ik_1x} + S^{(-)}e^{-ik_1x}}. \quad (38)$$

The element of the S matrix, $S^{(-)}$, can be obtained by solving this equation

$$S^{(-)} = e^{2ik_1x}\frac{\hbar k_1 - p(x)}{\hbar k_1 + p(x)}. \quad (39)$$

Therefore, we can choose a point far enough from the interaction region and calculate the reflection and transmission coefficients through $R=|S^{(-)}|^2$ and $T=1-R$.

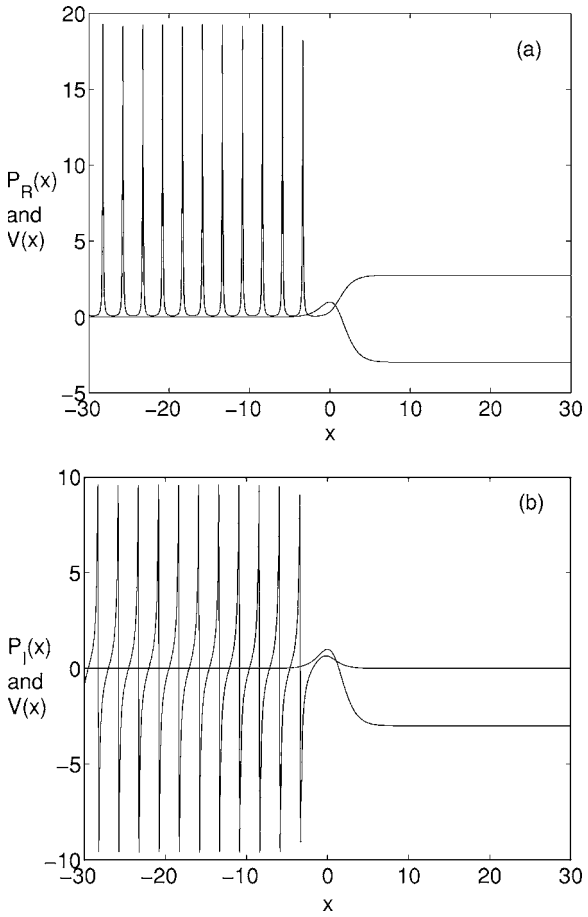

FIG. 6. Quantum momentum function (oscillating curve) and potential barrier ($c=0.5$): (a) Real part of momentum; (b) imaginary part of momentum.

C. Computational results: Probability density and quantum momentum function

We present the results obtained by numerically solving the QHJE for a one-dimensional potential barrier [34]:

$$V(x) = V_0\left[1 - \left(\frac{1-e^x}{1+ce^x}\right)^2\right], \quad (40)$$

where $0 \leqslant c \leqslant 1$. When $c=0$, this potential gives the Morse barrier, $V(x)=V_0(2\exp(x)-\exp(2x))$ and, when $c=1$, the potential gives the symmetric Eckart barrier, $V(x)=V_0\mathrm{sech}^2(x)$.

As an example, we set $\hbar=m=1$ and $c=0.5$. The barrier height V_0 is chosen to be 1 and the energy of the incident particle is 0.8. We integrate backwards using the second-order Möbius integrator (from $x=30$ to $x=-30$) to numerically obtain the QMF. The step size h is -0.01 and the number of steps is 6000. The wave function can be numerically obtained through the phase integral in Eq. (36) approximated by the trapezoidal rule.

The numerical results for the scattering problem are given in Figs. 5 and 6. The probability density and the potential barrier are shown in Fig. 5. The reflection and transmission coefficient are obtained through Eq. (39) by choosing $x=-30$. In this case, $R=0.7689404$ and $T=0.2310596$, and the

exact reflection and transmission coefficients are $R=0.7689360$ and $T=0.2310640$ [34]. These numerical results are in excellent agreement with the exact values.

In Fig. 6, the results for the real and imaginary parts of the QMF are shown. We can see that the pole structure for the real and imaginary parts of the QMF on the left side of the barrier are similar to those for the potential step problem in Sec. III. *Quasipoles* are formed on the real x axis and there are an infinite number of these on the left side of the barrier. Furthermore, there is no pole on the right side of the barrier and the QMF is pure real for the transmitted part. This feature arises from a wave traveling to the right with a constant momentum.

D. Comparison with the Numerov integrator

We will now compare the Möbius algorithm with a different integrator, the Numerov method [35]. The one-dimensional Schrödinger equation can be written in the form

$$\frac{d^2}{dx^2}\psi(x) + Q(x)\psi(x) = 0, \tag{41}$$

where $Q(x)=(2m/\hbar^2)[E-V(x)]$. The Numerov method is an efficient algorithm used to obtain numerical solutions of Eq. (41). The recursion formula for this method is

$$(1-T_{n+1})\psi_{n+1} - (2+10T_n)\psi_n + (1-T_{n-1})\psi_{n-1} = 0, \tag{42}$$

where $\psi_n=\psi(x_n)$ and $T_n=-(h^2/12)Q(x_n)$. Here h is again the step size between the grid points.

We have mentioned that the exact wave function approaches an outgoing plane wave when x goes to ∞. Therefore, we can choose an initial point x_i far enough from the interaction region, and use $\psi_1=\psi(x_i)=e^{ik_2x_i}$ and $\psi_2=\psi(x_i+h)=e^{ik_2(x_i+h)}$ as the two initial terms for the recursion formula in Eq. (42) to numerically integrate the Schrödinger equation backwards (the step size h is negative). After obtaining the numerical solutions in region I in Fig. 4, we can determine the reflection coefficient through the asymptotic form of the wave function in Eq. (37). We choose the last two grid points, x_f and x_f-h, far enough from the interaction region and calculate the relative magnitude of the wave function

$$\frac{\psi(x_f)}{\psi(x_f-h)} = \frac{e^{ik_1x_f} + S^{(-)}e^{-ik_1x_f}}{e^{ik_1(x_f-h)} + S^{(-)}e^{-ik_1(x_f-h)}}. \tag{43}$$

The element of the S matrix, $S^{(-)}$, can be obtained by solving this equation for $S^{(-)}$

$$S^{(-)} = \frac{re^{ik_1(x_f-h)} - e^{ik_1x_f}}{e^{-ik_1x_f} - re^{-ik_1(x_f-h)}}, \tag{44}$$

where $r=\psi(x_f)/\psi(x_f-h)$. Thus the reflection and transmission coefficients can be determined through $R=|S^{(-)}|^2$ and $T=1-R$.

For the Numerov method, the wave function is obtained from the recursion formula (42) and then the reflection and transmission coefficients are calculated by Eq. (44). In the approach described previously, the QMF is obtained first from the Möbius integrator and then the wave function is synthesized from the QMF. Although Eq. (44) can also be

TABLE I. The reflection coefficients for $V_0=1$.

c	E	h	R (Second)[a]	Error[c]	R (Fourth)[b]	Error[c]	R (Numerov)	Error[c]
1	1.2	−0.1	0.1220142	2.78×10^{-4}	0.1217361	-2.13×10^{-7}	0.1217356	-6.86×10^{-7}
		−0.05	0.1218059	6.96×10^{-5}	0.1217363	-1.33×10^{-8}	0.1217362	-4.25×10^{-8}
		−0.025	0.1217537	1.74×10^{-5}	0.1217363	-8.28×10^{-10}	0.1217363	-2.64×10^{-9}
		−0.0125	0.1217406	4.35×10^{-6}	0.1217363	-5.17×10^{-11}	0.1217363	-1.64×10^{-10}
	0.5	−0.1	0.9927525	-3.92×10^{-5}	0.9927917	8.65×10^{-9}	0.9927917	8.77×10^{-10}
		−0.05	0.9927819	-9.78×10^{-6}	0.9927917	5.34×10^{-10}	0.9927917	5.43×10^{-11}
		−0.025	0.9927892	-2.45×10^{-6}	0.9927917	3.32×10^{-11}	0.9927917	3.31×10^{-12}
		−0.0125	0.9927911	-6.11×10^{-7}	0.9927917	2.07×10^{-12}	0.9927917	1.18×10^{-13}
0.25	1.2	−0.1	0.2356730	7.59×10^{-4}	0.2349132	-8.41×10^{-7}	0.2350006	8.65×10^{-5}
		−0.05	0.2351049	1.91×10^{-4}	0.2349140	-5.22×10^{-8}	0.2349191	5.07×10^{-6}
		−0.025	0.2349618	4.78×10^{-5}	0.2349141	-3.25×10^{-9}	0.2349144	3.03×10^{-7}
		−0.0125	0.2349260	1.19×10^{-5}	0.2349141	-2.03×10^{-10}	0.2349141	1.84×10^{-8}
	0.5	−0.1	0.9548286	-3.15×10^{-6}	0.9548320	2.70×10^{-7}	0.9548227	-9.10×10^{-6}
		−0.05	0.9548305	-1.23×10^{-6}	0.9548318	1.69×10^{-8}	0.9548313	-4.93×10^{-7}
		−0.025	0.9548314	-3.34×10^{-7}	0.9548318	1.06×10^{-9}	0.9548317	-2.79×10^{-8}
		−0.0125	0.9548317	-8.49×10^{-8}	0.9548318	6.62×10^{-11}	0.9548318	-1.64×10^{-9}

[a]Second-order Möbius results.
[b]Fourth-order Möbius results.
[c]Error$(R)=R-R_{\text{exact}}$.

used to determine the reflection and transmission coefficients through the synthesized wave function, using Eq. (39) to obtain the reflection and transmission coefficients through the QMF avoids the numerical error from synthesis of the wave function.

In Table I, the reflection and transmission coefficients obtained from the second-order and fourth-order Möbius integrators for two different potential energy functions and scattering energies are shown for four values of the step size h. Additionally, the reflection and transmission coefficients obtained using the Numerov method (using $x_i=30$ and $x_f=-30$) are also shown in Table I. From this table, we can see that the fourth-order Möbius integrator used to obtain the reflection and transmission coefficients is as accurate as or even more accurate than the Numerov method.

E. Step size dependence and error analysis

It is worth mentioning that several approximations have been used in the whole computational process. First, the Möbius integrator was used to numerically solve the QHJE in Eq. (30). Then, we took the *asymptotic value* of the QMF $\hbar k_2$ as the initial condition at $x=b$ in Fig. 4; actually, this initial value is not exact (except when $x\to\infty$). Finally, the reflection and transmission coefficients were determined by Eq. (39) based on the assumption that the scattering wave function has the asymptotic form in Eq. (37) at $x=a$ in Fig. 4. Therefore, the overall error comes from the Möbius integrator and from truncation of the propagation region. Similarly, when the Numerov method was used to solve Eq. (41) for the whole process, the wave function was assumed to be the asymptotic forms e^{ik_2x} at $x=b$ to start the propagation and to be $e^{ik_1x}+S^{(-)}e^{-ik_1x}$ at $x=a$ to determine the reflection and transmission coefficients through Eq. (44). Although we did not present the error analysis for the whole computational process, it is expected that if the propagation region (a,b) is chosen to be sufficiently large, the errors from these asymptotic behaviors of the QMF and of the scattering wave function at the end points of the propagation region will be reduced.

The step size dependence of the error for both the Möbius and the Numerov integrators for the propagation region $(-30,30)$ is shown in Fig. 7. The error is assumed to have the form $|\text{Error}|=Ah^m$, where A is a constant. Therefore, the data were fit to the linear equation $\log_{10}|\text{Error}|=\log_{10}A+m\log_{10}h$ by the method of least squares. The errors are fit very well by this equation and values for the order m are given in the figure caption. We observe that the fourth-order Möbius integrators and the Numerov integrator achieve high accuracy when the step size is reduced. Even for $h=0.0125$, the reflection and transmission coefficients can have the accuracy of 10 decimal places.

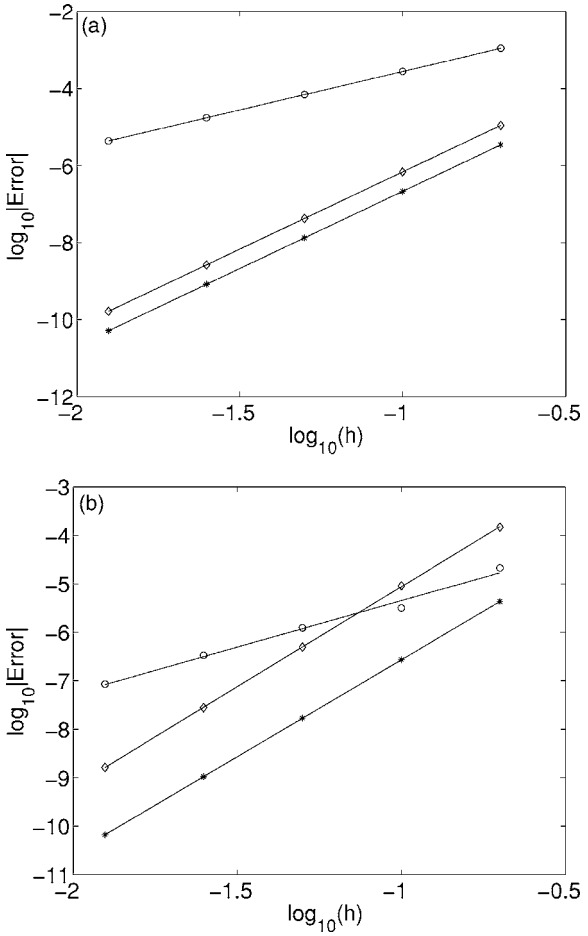

FIG. 7. Step size dependence of the error ($|\text{Error}|=Ah^m$) for $h=0.2$, 0.1, 0.05, 0.025, and 0.0125; Möbius integrator [second order (○); fourth order (∗)] and Numerov integrator (◇). (a) $E=1.2$, $V_0=1$, and $c=1$: second order $m=1.996$; fourth order $m=4.008$; Numerov $m=4.009$; (b) $E=0.5$, $V_0=1$, and $c=0.25$: second order $m=1.919$; fourth order $m=3.995$; Numerov $m=4.126$.

V. SUMMARY AND CONCLUSION

In this study, a computational method for the QHJE for general one-dimensional scattering problems was proposed. This method was demonstrated for a potential barrier problem. We first briefly reviewed the quantum Hamilton-Jacobi formalism. The pole structure of the QMF for scattering wave functions was thoroughly analyzed for the potential step. The QMF of scattering wave functions generally has poles in the complex plane and for some cases, there are an infinite number of poles on the real axis. Additionally, when these poles are very close to the real axis, the QMF shows the "*quasipole*" structure before the exact poles form on the real axis. Then, we proposed an accurate computational procedure for general one-dimensional scattering problems to obtain the wave function and the reflection and transmission coefficients. For an arbitrary localized potential, we started the integration of the QHJE for the QMF at a large positive value of x in the transmitted region, and integrated backwards. Subsequently, the QMF was used to determine the reflection and transmission coefficients and the wave function was synthesized through the phase integral. Not only can we obtain the numerical solution of the QMF through the computational approach, but it is also simple to reconstruct the reflection coefficient from the QMF. Furthermore, the computational results obtained from the fourth-order Möbius integrator can achieve very high accuracy.

It has been demonstrated in this study that this computational method for the QHJE is suitable for general one-dimensional scattering systems. This study not only has presented an alternative method to the numerical solution of the wave function and the reflection and transmission coefficients for one-dimensional scattering problems but also has provided an accurate computational aspect within the quantum Hamilton-Jacobi formalism. In addition, use of the Möbius propagation method for the QHJE has also been applied to one-dimensional bound state problems [33]. Further analysis and applications for multidimensional problems will be reported in our future studies.

ACKNOWLEDGMENT

We thank the Robert Welch Foundation for their financial support of this research.

[1] R. A. Leacock and M. J. Padgett, Phys. Rev. Lett. **50**, 3 (1983).
[2] R. A. Leacock and M. J. Padgett, Phys. Rev. D **28**, 2491 (1983).
[3] R. S. Bhalla, A. K. Kapoor, and P. K. Panigrahi, Am. J. Phys. **65**, 1187 (1997).
[4] R. S. Bhalla, A. K. Kapoor, and P. K. Panigrahi, Mod. Phys. Lett. A **12**, 295 (1997).
[5] S. S. Ranjani, K. G. Geojo, A. K. Kapoor, and P. K. Panigrahi, Mod. Phys. Lett. A **19**, 1457 (2004).
[6] S. S. Ranjani, A. K. Kapoor, and P. K. Panigrahi, Mod. Phys. Lett. A **19**, 2047 (2004).
[7] S. S. Ranjani, A. K. Kapoor, and P. K. Panigrahi, Ann. Phys. (N.Y.) **320**, 164 (2005).
[8] S. S. Ranjani, A. K. Kapoor, and P. K. Panigrahi, Int. J. Theor. Phys. **44**, 1167 (2005).
[9] C. Rasinariu, J. J. Dykla, A. Gangopadhyaya, and J. V. Mallow, Phys. Lett. A **338**, 197 (2005).
[10] R. S. Bhalla, A. K. Kapoor, and P. K. Panigrahi, Int. J. Mod. Phys. A **12**, 1875 (1997).
[11] R. S. Bhalla, A. K. Kapoor, and P. K. Panigrahi, Phys. Rev. A **54**, 951 (1996).
[12] K. G. Geojo, S. S. Ranjani, and A. K. Kapoor, J. Phys. A **36**, 4591 (2003).
[13] M. V. John, Found. Phys. Lett. **15**, 329 (2002).
[14] C.-D. Yang, Ann. Phys. (N.Y.) **319**, 339 (2005).
[15] C.-D. Yang, Int. J. Quantum Chem. **106**, 1620 (2006).
[16] C.-D. Yang, Ann. Phys. (N.Y.) **319**, 444 (2005).
[17] C.-D. Yang, Chaos, Solitons Fractals **30**, 342 (2006).
[18] D. J. Tannor, *Introduction to Quantum Mechanics: A Time-Dependent Perspective* (University Science Books, Sausalito, 2006).
[19] Y. Goldfarb, I. Degani, and D. J. Tannor, e-print quant-ph/0604150
[20] E. R. Floyd, Phys. Rev. D **26**, 1339 (1982).
[21] E. R. Floyd, Phys. Rev. D **29**, 1842 (1984).
[22] E. R. Floyd, Phys. Rev. D **34**, 3246 (1986).
[23] E. R. Floyd, Found. Phys. Lett. **9**, 489 (1996).
[24] A. E. Faraggi and M. Matone, Int. J. Mod. Phys. A **15**, 1869 (2000).
[25] B. Poirier, J. Chem. Phys. **121**, 4501 (2004).
[26] C. Trahan and B. Poirier, J. Chem. Phys. **124**, 034115 (2006).
[27] C. Trahan and B. Poirier, J. Chem. Phys. **124**, 034116 (2006).
[28] C.-D. Yang, Chaos, Solitons Fractals **32**, 312 (2007).
[29] J. Schiff and S. Shnider, SIAM (Soc. Ind. Appl. Math.) J. Numer. Anal. **36**, 1392 (1999).
[30] N. Zettili, *Quantum Mechanics: Concepts and Applications* (John Wiley & Sons, Chichester, 2001).
[31] L. V. Ahlfors, *Complex Analysis* (McGraw-Hill, New York, 1979).
[32] C. H. Chang and J. H. Wang, Comput. Phys. Commun. **69**, 330 (1992).
[33] C.-C. Chou and R. E. Wyatt, J. Chem. Phys. **125**, 174103 (2006).
[34] Z. Ahmed, Phys. Rev. A **47**, 4761 (1993).
[35] J. M. Blatt, J. Comput. Phys. **1**, 382 (1967).